

Structure-sensitive investigations on glass fibers from the system $\text{SiO}_2\text{-Al}_2\text{O}_3\text{-CaO}$

Jürgen Murach¹⁾, Andreas Makat and Rolf Brückner

Institut für Nichtmetallische Werkstoffe, Technische Universität Berlin (Germany)

Glass fibers of the system $\text{SiO}_2\text{-Al}_2\text{O}_3\text{-CaO}$ were prepared with respect to defined drawing conditions and investigated with structure-sensitive methods (birefringence, radial and axial alterations by thermal treatment at T_g). These glass fibers, which lie in a compositional sense roughly between the disilicate and silica glasses concerning the ratio network modifiers to network formers, exhibit similar optical anisotropies. On the other hand, they show remarkably lower axial and radial alterations which are exclusively contractions on annealing for all applied drawing conditions in contrast to the silica or the alkali disilicate glass fibers. Obviously, the filling of free volume hollows with and the reinforcement of them by the Ca^{2+} ions and the smaller polarizability of the latter as compared to alkali ions are responsible for the relatively low structural anisotropy. An increase of the optical anisotropy with increasing CaO concentration is observed at comparable viscosities. This is a consequence of the increasing incorporation of the network modifier oxide which produces a weaker network strength and a larger polarizability.

Struktursensitive Untersuchungen an Glasfasern aus dem System $\text{SiO}_2\text{-Al}_2\text{O}_3\text{-CaO}$

Es wurden Glasfasern des Systems $\text{SiO}_2\text{-Al}_2\text{O}_3\text{-CaO}$, nach dem Düsenziehverfahren unter verschiedenen, definierten Ziehbedingungen hergestellt und mit struktursensitiven Methoden untersucht (Doppelbrechung, radiale und axiale Veränderungen durch thermische Behandlung bei T_g). Diese Glasfasern, die bezüglich ihres Netzwerkmodifizier-/Netzwerkbildnerverhältnisses zwischen den Disilicat- und den Kieselgläsern liegen, weisen ähnliche optische Anisotropien wie diese auf. Andererseits liegen auffallend niedrigere Werte der axialen und radialen Veränderungen vor, wobei die Glasfasern beim Tempern für alle Ziehbedingungen im Gegensatz zu den Kieselgläsern und den Disilicatglasfasern sowohl in axialer als auch in radialer Richtung ausschließlich kontrahieren. Verantwortlich für diese relativ geringe strukturelle Anisotropie sind offenbar die Auffüllung des freien Hohlraumvolumens und dessen Verfestigung durch die Ca^{2+} -Ionen sowie die geringe Polarisierbarkeit der Ca^{2+} -Ionen im Vergleich zu den Alkali-Ionen. Bezogen auf die gleiche Viskosität kann bei den untersuchten Glasfasern eine deutliche Zunahme der optischen Anisotropie mit steigendem CaO-Gehalt festgestellt werden. Dies ist die Folge der zunehmenden Inkorporation des Netzwerkmodifizieroxides, die eine geringere Netzwerkfestigkeit und größere Polarisierbarkeit erzeugt.

1. Introduction and objective

In former investigations of structure-sensitive properties of glass fibers with compositions for model glasses, conclusions could be drawn on the structure of glasses, glass melts and glass fibers. The investigations included alkali- and alkaline metaphosphate glass fibers [1 to 3] as well as silicate glass fibers with compositions between alkali metasilicate and pure silica [4 and 5]. The purpose of this study is to extend the investigations to another alkali- and boron oxide-free aluminosilicate group of glasses which has been investigated recently under different practical and theoretical aspects [6]. Particularly the variation of chemical composition should give information about the role of CaO and Al_2O_3 when incorporated into the network.

2. Selected glass compositions and experimental

Three compositions from the system $\text{SiO}_2\text{-Al}_2\text{O}_3\text{-CaO}$ were selected. Starting from the eutectic composition of

this system the content of CaO was increased at the expense of Al_2O_3 or SiO_2 (table 1.). Further investigations could not be realized because the fibers of glass no. 4 crystallized during the fiber drawing process.

The glass fibers were produced by the nozzle drawing method described in [3], which allows a good separation of the structure-determining parameters. The contraction (shrinking) of the fiber bundles during heating and annealing at T_g could be measured for all drawing conditions by means of a differential dilatometer. The annealing at T_g for the total relaxation of the fiber bundles took 15 h.

3. Results

Table 1 characterizes the annealed glasses with respect to T_g and density at room temperature. A more important property is the temperature dependence of viscosity within the range of spinnability. This was measured with a cylinder rotation viscometer. Figure 1 shows the results. At constant temperatures the viscosities decrease continuously from the glass melts nos. 1 to 4. The upper temperature limit of spinnability was given for all glass

Received 14 January 1998.

¹⁾ Now with: Senat von Berlin, Berlin (Germany)

Table 1. Compositions of the investigated glasses and fibers in mol%, T_g and density at room temperature

glass nos.	Composition in mol%					T_g in °C	density in g/cm ³
	SiO ₂	Al ₂ O ₃	CaO	CaO/Al ₂ O ₃	SiO ₂ /CaO		
1	65	9	26	2.9	2.50	787	2.6220
2	65	5	30	6.0	2.17	784	2.6428
3	58	9	33	3.7	1.76	779	2.7216
4	53	9	38	4.2	1.39	773	2.7622

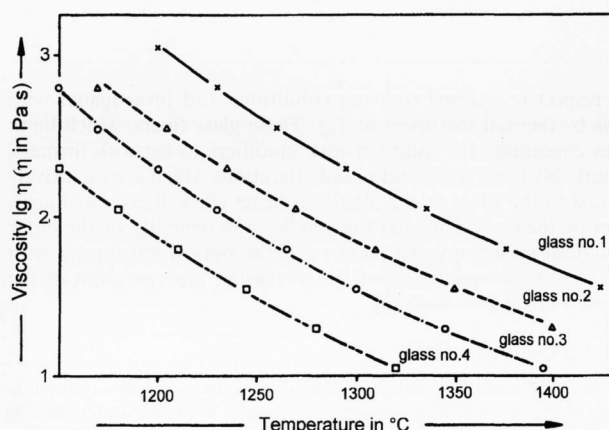
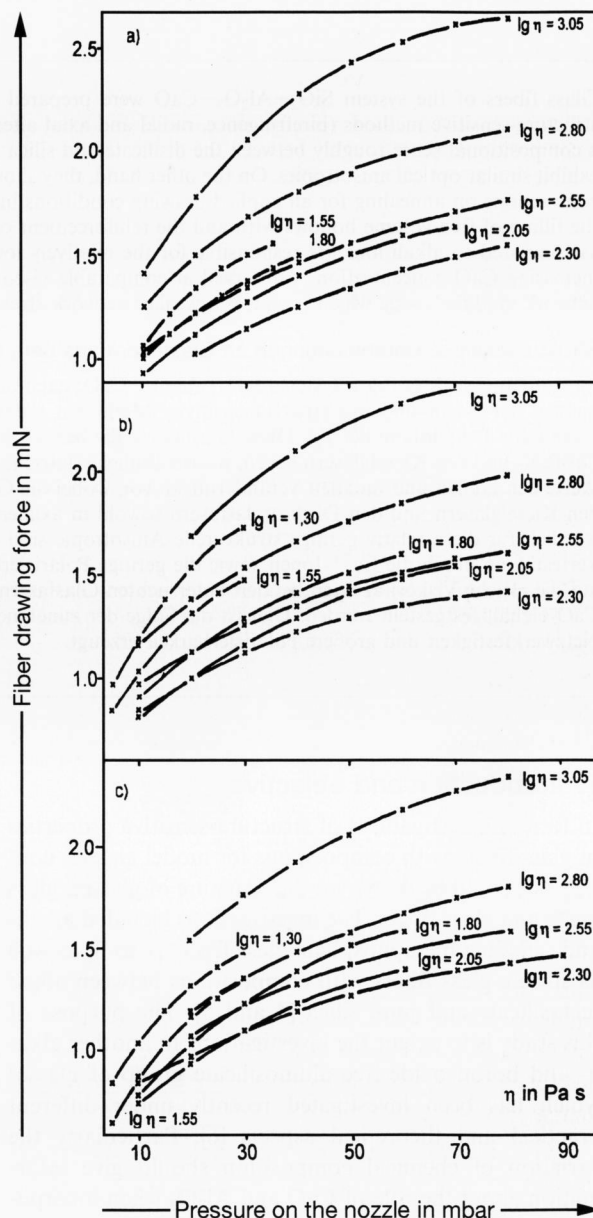


Figure 1. Viscosity-temperature curves of glasses nos. 1 to 4 of the system SiO₂-Al₂O₃-CaO.

melts by the nozzle drawing equipment at 1420°C. Thus, viscosity values could be realized for glass no. 1 only for $\lg \eta > 1.55$ (η in Pa s). The lower temperature limit was between 1180 to 1230°C depending on glass composition and drawing condition.

Figures 2a to c show the results of the measurements of the fiber drawing force depending on the pressure on the nozzle and on the viscosity of the melt in the nozzle. The minimum of the drawing force, caused by wetting the nozzle end face area, is between $\lg \eta = 2.05$ and 2.30 (η in Pa s) and is shifted to larger viscosities as compared to mixed-alkali silicate glasses ($\lg \eta = 1.9$) for the metasilicate glass [3]. This indicates that also the optimum of the drawing temperature is shifted in a similar manner. At higher temperatures or lower viscosities than $\eta = 10^2$ Pa s large oscillations occurred which led to interruptions of the fiber drawing process.

The fiber drawing temperatures of the glass melts nos. 1 to 3 were selected in such a way that equal viscosities existed for the measurements of the birefringence as a function of the drawing stress. Thus, the frozen-in stress-optical constants (= apparent stress-optical constants) of the fibers nos. 1 to 3 were measured at viscosities $\lg \eta = 2.30, 2.80$ and 3.05 (η in Pa s). The result is seen in figure 3. The apparent stress-optical constant, $C^* = \Delta n / \Delta \sigma_z$, increases with increasing temperature (decreasing viscosity). Similar to silica and disilicate glass fibers [4 and 5] the temperature dependence of the



Figures 2a to c. Fiber-drawing force as a function of the pressure on the nozzle at various viscosities in the nozzle (η in Pa s); a) glass melt no. 1, b) glass melt no. 2, c) glass melt no. 3.

apparent stress-optical constant (or birefringence) is relatively weak as compared to the alkali metasilicate and metaphosphate glass fibers [1 to 3]. The C^* values also

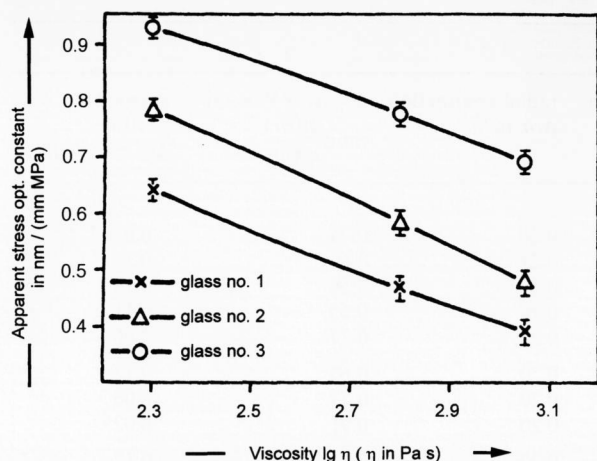


Figure 3. Apparent (frozen-in) stress optical constant versus \lg viscosity for glass fibers nos. 1 to 3.

increase with increasing CaO concentration. The values of the glass fibers no. 1 with 26 mol% CaO are between 0.4 and 0.65 nm/(mm MPa) and are corresponding with those of silica glass fibers produced from "Suprasil" [4].

The increase in CaO at the expense of Al_2O_3 leads to an increase in C^* (glass no. 2). Obviously, Al_2O_3 plays the role of a network former in this composition range. The increase of CaO up to 7 mol% at the expense of SiO_2 (glass no. 3) leads to still higher values of C^* which are up to nearly 1.0 nm/(mm MPa).

The values of axial shrinkage of the fibers for the glasses nos. 1 to 3 (figure 4) are significantly smaller than those for the alkali silicate glass series [5]. The maximum shrinkage values are only about 0.5% for fibers with 10 μm diameter. Silica glass fibers show axial contraction values which are more than the double of those shown in figure 4 at comparable conditions. During these measurements the thermal history was kept constant ($2R = 10 \mu\text{m}$, $\lg \eta = 3.05$, η in Pa s). It is seen from figure 4 that an increase of CaO content at the expense of SiO_2 or Al_2O_3 leads mainly to a change of the isotropic portion of shrinkage (values at $\sigma_z = 0$), while the slopes of the straight lines ($\Delta l/l = f(\sigma_z)$) are changed only to a small degree. Figure 5 shows the fiber shrinkage, $\Delta l/l$, versus drawing stress at various viscosities (temperatures) for glass fibers no. 1 with a constant diameter of 10 μm .

As in the case of the di- and metasilicate glasses the fiber-drawing process leads to a decrease in the density (figure 6) within a range of 0.5 and 0.9%. The decrease in the density decreases with increasing CaO concentration. This may be explained in two ways: the drawing temperature decreases at equal viscosities and with this also the quenching rate. But it may also be possible that the filling of the free volume hollows with Ca^{2+} ions leads to a stronger bonding of the network as compared to that with alkali ions and by that to less deformability of the network.

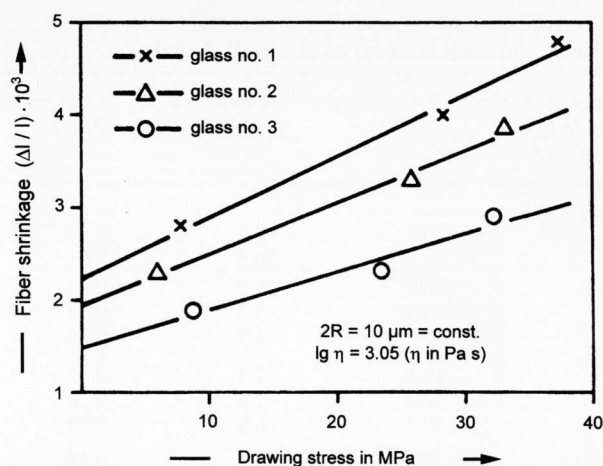


Figure 4. Axial fiber shrinkage by annealing versus drawing stress at constant viscosity ($\eta = 10^{3.05}$ Pa s) and constant fiber diameter ($2R = 10 \mu\text{m}$).

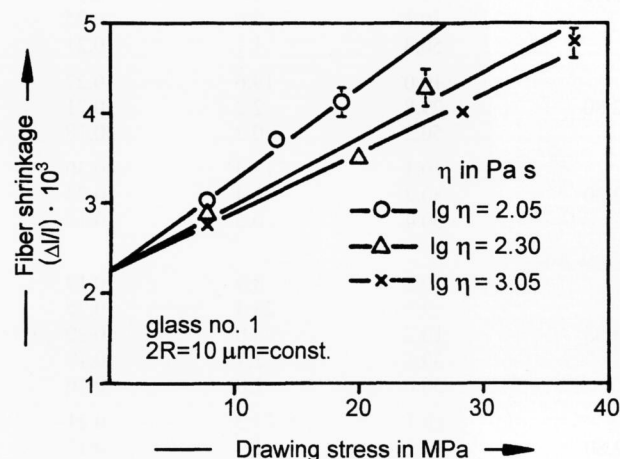


Figure 5. Axial fiber shrinking by annealing versus drawing stress for glass fibers no. 1 at various viscosities and constant fiber diameter ($2R = 10 \mu\text{m}$).

With the help of the density and axial shrinking the radial change of the fibers can be calculated as was done in [1 and 3 to 5]. Table 2 shows the results and additionally the values of the apparent Poisson ratio and the portion of anisotropy of the glass fibers nos. 1 to 3. The values indicate that the glass fibers with those chemical compositions are shrinking not only in axial but also in radial direction by annealing, while silica glass fibers expand exclusively in radial direction [4].

4. Discussion

The glass fibers of the system $\text{SiO}_2\text{-Al}_2\text{O}_3\text{-CaO}$ show an opposite behavior to formerly investigated glass fibers of the system $\text{SiO}_2\text{-R}_2\text{O}$ in such a manner that they are shrinking in axial and radial direction during annealing for all drawing conditions, i.e. the sign of $\Delta r/r$ in table 2 and that of the Poisson ratio is positive in all cases. It is also remarkable that the anisotropic por-

Table 2. Shrinking behavior of fibers nos. 1 to 3

viscosity in the nozzle $\lg \eta$ (η in Pa s)	fiber diameter in μm	drawing stress in MPa	axial contraction $\Delta l/l$ in %	radial contraction $\Delta r/r$ in %	apparent Poisson ratio $\frac{(\Delta r/r)}{(\Delta l/l)}$	anisotropic portion $\Delta l/l - \Delta r/r$ in %
<u>glass no. 1.</u>						
	10.1	8.1	0.27	0.20	0.74	0.07
	10.0	20.5	0.35	0.21	0.60	0.14
3.05	10.0	26.2	0.41	0.22	0.54	0.19
	30.1	3.2	0.31	0.20	0.65	0.11
	49.8	1.2	0.26	0.20	0.77	0.06
	10.1	21.5	0.32	0.20	0.63	0.12
2.80	30.0	2.4	0.26	0.20	0.77	0.06
	50.1	0.9	0.22	0.20	0.91	0.02
	10.2	13.2	0.37	0.20	0.54	0.17
2.30	30.3	1.5	0.29	0.20	0.69	0.09
	49.9	0.5	0.24	0.20	0.83	0.04
<u>glass no. 2</u>						
	10.1	5.9	0.19	0.17	0.89	0.02
	10.2	26.5	0.33	0.19	0.58	0.14
3.05	9.9	33.8	0.39	0.21	0.54	0.18
	30.1	3.0	0.25	0.18	0.72	0.07
	50.3	1.1	0.21	0.18	0.86	0.03
	10.0	19.6	0.27	0.17	0.63	0.10
2.80	29.8	2.2	0.21	0.17	0.81	0.04
	50.2	0.8	0.18	0.17	0.94	0.01
	10.1	12.4	0.30	0.18	0.60	0.12
2.30	30.2	1.4	0.23	0.17	0.74	0.06
	50.4	0.5	0.19	0.18	0.95	0.01
<u>glass no. 3</u>						
	10.2	8.9	0.19	0.16	0.84	0.03
	9.9	23.4	0.25	0.17	0.68	0.08
3.05	10.2	33.0	0.29	0.19	0.66	0.10
	30.1	2.7	0.19	0.16	0.84	0.03
	50.0	1.0	0.16	0.16	1.00	0.00
	10.1	17.2	0.21	0.18	0.86	0.03
2.80	30.2	1.9	0.17	0.18	1.06	-0.01
	49.7	1.7	0.14	0.16	1.14	-0.02
	10.1	12.0	0.27	0.18	0.66	0.09
2.30	30.3	1.4	0.21	0.16	0.76	0.05
	49.9	0.5	0.18	0.16	0.89	0.02

tion, calculated from the difference of axial and radial shrinkage, is extremely smaller, i.e. by one order of magnitude smaller than the values for the silica- and disilicate glass fibers, while the values of the apparent stress-optical constants are in the same order of magnitude as those for the disilicate glass fibers [4 and 5].

Of special interest is the comparison of the values of table 2 with corresponding values for E-glass fibers [7], because these are also alkali-free and their second and third main components are also CaO and Al_2O_3 , and because the axial and radial shrinkage as well as the apparent Poisson ratio and the anisotropic portion are in the same order of magnitude as for the present fibers. The overall positive sign of $\Delta r/r$ is also characteristic of the two glass fiber types.

The results of the structure-sensitive measurements of the present fibers give rise to the following interpretation:

- The Al_2O_3 acts as a network former oxide with AlO_4 tetrahedra due to the CaO concentration. This agrees with NMR-MAS investigations of Engelhard et al. [8] on ^{29}Si and ^{27}Al .
- The increase in the CaO content results in two effects; first, the network modifier portion is increased and therefore the apparent stress-optical constant is increased by the larger polarizability of the Ca^{2+} ions compared with that of the Al^{3+} and Si^{4+} as well as of the nonbridging oxygen ions. Second, on the other hand, the Ca^{2+} ions fill the free volume hollows of the network

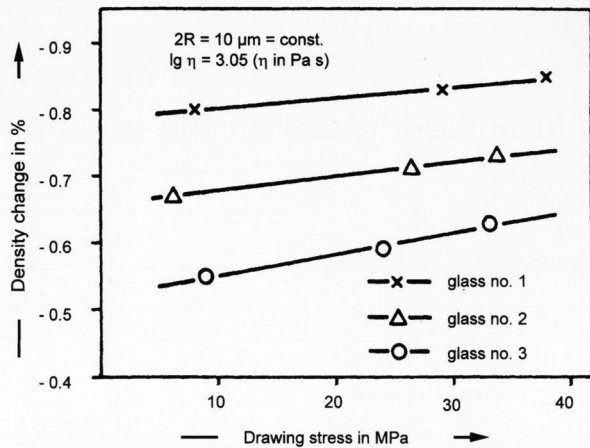


Figure 6. Change of the density for glass fibers nos. 1 to 3 versus drawing stress at constant thermal history, i.e. at constant viscosity ($\eta = 10^{3.05}$ Pa s) and constant fiber diameter ($2R = 10 \mu\text{m}$).

and make it stiffer and less deformable than that of the silica glass for instance, with the consequences that the axial shrinkage values are so small, that $\Delta r/r$ is always positive, and the anisotropic portion is so small, too.

This leads to the conclusion that orientation phenomena in fibers of the present glass system are so small, that they atrophy to small network deformation. The extremely high positive values of the apparent Poisson ratio, $\mu^* = (\Delta r/r)/(\Delta l/l)$, which are sometimes larger than 1.0, indicate that the thermal history of the fibers (T and $\dot{T} = dT/dt$) dominates by far the mechanical history (drawing stress). The reason for this is again the very large stiffness of the network, which does not allow any structural orientations except those of Griffith's microcracks. To illustrate this with respect to μ^* , the following explanations may be given:

- $\mu^* = 0$ means $\Delta r/r = 0$, i.e., neither contraction nor expansion in radial direction on annealing;
- $0 > \mu^* < 0.5$ means radial shrinkage, $\Delta r/r$, is less than half of $\Delta l/l$ on annealing;
- $\mu^* = 0.5$ means that radial shrinkage, $\Delta r/r$, is accidentally half of $\Delta l/l$ on annealing;
- $\mu^* = 1.0$ means isotropic shrinking, $\Delta r/r = \Delta l/l$ i.e. pure thermal history, fibers do not show any reaction of mechanical history;
- $\mu^* > 1.0$ means $\Delta r/r > \Delta l/l$ i.e. thermal anisotropy, when quenching rate is larger in radial than in axial direction;
- $\mu^* < 0$ means $\Delta l/l > 0$ and $\Delta r/r < 0$, axial shrinkage and radial expansion; i.e. mechanical history clearly dominates thermal history. This indicates orientation effects and/or large deformations.

Addresses of the authors:

Jürgen Murach
Senatsverwaltung f. Bauen, Wohnen u. Verkehr
An der Urania 4-10
D-10787 Berlin

Andreas Makat
Institut f. Nichtmetallische Werkstoffe
Technische Universität
Englische Straße 20
D-10587 Berlin

R. Brückner
Fritz-Müller-Straße 57
D-82467 Garmisch-Partenkirchen

It is seen that the apparent Poisson ratio, μ^* , has only little to do with the usual Poisson ratio, $\mu = (\Delta r/r)/(\Delta l/l) = \epsilon_r/\epsilon_l$ with values between 0 and 0.5 for the isotropic-pure elastic body ($\mu = 0.5$) and the totally deformable body without radial deformation ($\mu = 0 = \Delta r/r$). But μ^* gives a good measure for the structural response to frozen-in deformations like that of the fiber produced by drawing procedures. This is visible not only from this article (table 2), but also from similar investigations as already mentioned above [1 and 3 to 7].

5. Conclusion

It is shown that glass fibers of the system $\text{SiO}_2\text{-Al}_2\text{O}_3\text{-CaO}$ exhibit the lowest degree of structural anisotropy as compared with fibers of metaphosphate, metasilicate, disilicate and even of silica glass. This is not only due to the three-dimensionally connected $\text{SiO}_2\text{-Al}_2\text{O}_3$ network structure but also a consequence of a low degree of free volume due to the Ca^{2+} ions which are filling, at least partly, this volume. This makes the network stiffer than the SiO_2 network and therefore the properties of the here investigated fibers are more related to the E-glass fibers which, however, indicate a somewhat higher degree of structural anisotropy.

6. References

- [1] Stockhorst, H.; Brückner, R.: Structure sensitive measurements on phosphate glass fibers. *J. Non-Cryst. Solids* **85** (1986) p. 105-126.
- [2] Stockhorst, H.; Brückner, R.: Stress optical investigations of glass fibres with linearly and three-dimensionally branched networks. *Phys. Chem. Glasses* **27** (1986) no. 5, p. 204-209.
- [3] Murach, J.; Brückner, R.: Structure-sensitive investigations on alkali metasilicate glass fibers. *J. Non-Cryst. Solids* **204** (1996) p. 282-293.
- [4] Murach, J.; Brückner, R.: Preparation and structure-sensitive investigations on silica glass fibers. *J. Non-Cryst. Solids* **211** (1997) p. 250-261.
- [5] Murach, J.; Jander, S.; Brückner, R.: Structure-sensitive investigations on alkali-disilicate glass fibers with reference to metasilicate- and silica glass fibers. *J. Non-Cryst. Solids* **217** (1997) p. 92-98.
- [6] Kim, Y. K.; Brückner, R.; Murach, J.: Properties of textile glass fibers based on alkali- and boron oxide-free aluminosilicate glasses. *Glastech. Ber. Glass Sci. Technol.* **71** (1998) no. 3, p. 67-74.
- [7] Stockhorst, H.; Brückner, R.: Structure sensitive measurements on E-glass fibers. *J. Non-Cryst. Solids* **49** (1982) p. 471-484.
- [8] Engelhardt, G.; Nofz, M.; Forkel, K. et al.: Structural studies of calcium aluminosilicate glasses by high resolution solid state ^{29}Si and ^{27}Al magic angle spinning nuclear magnetic resonance. *Phys. Chem. Glasses* **26** (1985) no. 5, p. 157-165.

■ 1198P002